YBCO Superconducting Ring Resonators at Millimeter-Wave Frequencies

Christopher M. Chorey, *Member, IEEE*, Keon-Shik Kong, *Student Member, IEEE*, Kul B. Bhasin, *Senior Member, IEEE*, J. D. Warner, and Tatsuo Itoh, *Fellow, IEEE*

***Abstract*— Superconducting microstrip ring resonators operating at 35 GHz have been fabricated from laser ablated $YBa_2Cu_3O_{7-x}$ (YBCO) films on lanthanum aluminate substrates. The circuits consist of superconducting strips over normal metal ground planes. The circuits are measured from 20 K to 90 K and with microwave input powers ranging from 0.25 mW to 10 mW. The superconducting resonators show significant improvement in Q (six to seven times higher) over identical gold resonators at 20 K, but only marginal improvement at 77 K. No variation in the superconductor performance is observed with varying input power. Using a microstrip loss model, the microwave surface resistance of the superconductors is extracted; the lowest value obtained at 77 K is 9 mΩ. The change in the resonant frequency with temperature is analyzed and a value for the penetration depth computed. "Double resonances" observed in some superconducting ring resonators are described and an explanation for their presence advanced. Factors limiting millimeter-wave high-temperature superconductor circuits are explored and potential performance levels calculated based on current reported values for high-temperature superconductor surface resistances.**

I. Introduction

Continued refinement in the growth of thin high-temperature superconducting (HTS) $YBa_2Cu_3O_{7-x}$ (YBCO) films on microwave-suitable substrates has resulted in materials with very low microwave losses. Currently, the best reported films have surface resistivities in the range of 0.1 mΩ at 77 K and 10 GHz [1]. When extrapolated assuming an f^2 dependence, surface resistivities lower than that of copper are seen to be possible to beyond 100 GHz. The availability of such low-loss films has spurred interest in microwave applications for these films. Frequently mentioned examples of where high-temperature superconductors could have an impact are microstrip filters [2], delay lines, and feed networks for monolithic antenna arrays [3] where overall circuit and system performance may be improved by the low-loss superconducting lines.

The microwave loss of the superconducting films is generally measured by one of several techniques, which may be grouped into two categories: 1) those that do not require patterning of the film, such as cavity techniques [4] or microwave transmission studies [5], and 2) those that pattern the film into some form of planar transmission line resonator [6]. Measurements on the patterned films are believed to give a more complete assessment of the superconductor performance in planar microwave circuits since factors such as dielectric loss, substrate/film interface imperfections, and edge damage caused by patterning are included in the response of the circuit. Such patterned film techniques have a drawback, however, in that values of the surface resistance (R_s) are difficult to extract, and the circuit Q values have little importance in comparisons between different test circuits. Nevertheless, these techniques, when coupled with reasonable attempts at modeling, can provide valuable insight into HTS microwave circuit performance.

A number of HTS surface resistance measurements exist ranging from 1 to 100 GHz [1]; these represent both cavity-type and patterned resonator measurements, although patterned resonator measurements are generally restricted to below 15 GHz. Because the superconductor's surface resistance increases as the frequency squared, smaller relative improvements over normal metals are expected as the frequency increases. Measurements on patterned resonators at millimeter-wave frequencies are therefore of interest in assessing the performance level possible when high-temperature superconductors are used at these frequencies and in determining the factors that limit such circuits' performance.

In this paper, we present results from the study of microstrip ring resonators at 35 GHz. These resonators were fabricated from single-sided YBCO films deposited by laser ablation on lanthanum aluminate ($LaAlO_3$). The response of the resonator was observed as a function of temperature, noting the resonator Q and the resonant frequency as well as the effect of the microwave drive power on the circuit performance. The results were compared with a gold implementation of the circuit. In addition to the comparison with the gold circuit, a microstrip loss model, the phenomenological loss equivalence method (PEM) was used to calculate surface resistances for the HTS films and an effective superconducting penetration depth was calculated. The factors limiting the circuit performance are discussed, and with the aid of the best published values for the superconducting surface resistance, potential circuit performance levels are calculated.

Manuscript received November 19, 1990; revised April 25, 1991.
C. M. Chorey is with the LeRC Group, Sverdrup Technology, 2001 Aerospace Parkway, Brook Park, OH 44142.
K. S. Kong is with the Electrical and Computer Engineering Department, University of Texas at Austin, Austin, TX 78712.
K. B. Bhasin and J. D. Warner are with the NASA Lewis Research Center, 21000 Brookpark Rd., Cleveland, OH 44135.
T. Itoh was with the Electrical and Computer Engineering Department, University of Texas at Austin. He is now with the Department of Electrical Engineering, UCLA, Los Angeles, CA 90024.
IEEE Log Number 9101199.

0018-9480/91/0900-1480$01.00

II. Circuit Fabrication and Testing

A. Film Growth and Patterning

The superconducting YBCO films used in this study were produced by laser ablation of a $YBa_2Cu_3O_{7-x}$ (YBCO) target onto one side of a heated lanthanum aluminate substrate. A 248 nm pulsed excimer laser with a pulse rate of 2 pps and a laser fluence of 2 J/cm^2 was used to ablate a $YBa_2Cu_3O_{7-x}$ stoichiometric pellet with a density of 95% of theoretical. The laser was rastered over the target by means of an external lens, and the deposition rate was approximately 100 Å per minute. The substrates were mounted on a heated (~ 755° C) stainless steel block 7.5 cm from the target and exposed to an ambient oxygen atmosphere of 170 mtorr during deposition. Following deposition, the oxygen pressure was raised to 1 atm, the block temperature lowered to 450° C, and the sample allowed to anneal at that temperature for two hours. Then the block was slowly cooled in oxygen to room temperature before removing the sample from the growth chamber. Film thicknesses were typically in the range of 3000 Å to 6000 Å and substrates slightly in excess of 1 cm^2 could be covered.

When observed in an optical or scanning electron microscope, the samples were generally found to be smooth and featureless but occasional surface roughness or particulates from the ablation process could be found. No misaligned platelets or indications of second phases were found in these examinations. X-ray diffraction analysis of the samples confirmed that to within the test resolution, the material was *c*-axis aligned and free of secondary phases. Transition temperatures (T_c) of up to 90 K were achieved.

The superconducting films were patterned into resonators by wet etching and standard photolithography. A positive photoresist was spun on, exposed, and developed in normal processing fashion. The films were then etched in a dilute solution of phosphoric acid in water (1:100::H_2O:H_3PO_4). The etch was quick, but undercutting was found to be minimized by the use of the very dilute solutions. Following etching, the photoresist was stripped in acetone. Since the samples had superconducting films on only one side of the substrate, a normal metal ground plane was evaporated to complete the circuit. First, 100 Å of titanium was deposited to promote adhesion of the gold layer, which was then evaporated. The ground plane thickness was slightly in excess of 1 μm.

B. Circuit Testing

The resonant circuit consisted of a microstrip ring with a 3λ resonance near 35 GHz; it is shown schematically in Fig. 1. The strip width was 143 μm and the mean diameter of the ring was 1980 μm. The ring was coupled to a single microstrip feed line via a capacitive gap 47 μm across. The substrate thickness was 254 μm (10 mils) to avoid substrate modes at 35 GHz. A normal metal ground plane was used and its thickness was 1 μm. Calculations

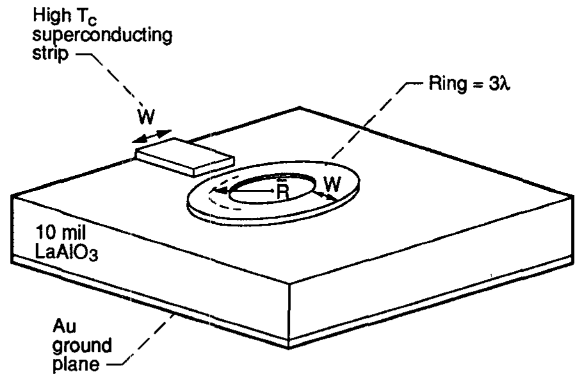

Fig. 1. A schematic drawing of the circuit used in this study. The microstrip ring was three wavelengths in circumference at 35 GHz. The line width was 143 μm and the substrate thickness 254 μm. The calculated line impedance was 38 Ω.

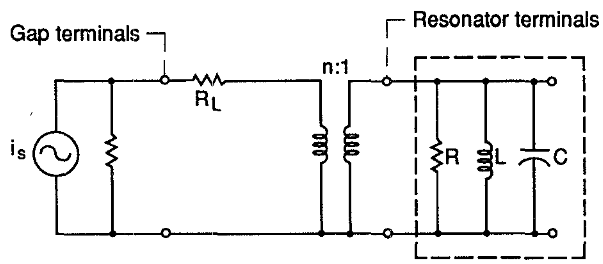

Fig. 2. The circuit model used to extract the unloaded *Q*. The coupling gap between the ring and feedline is modeled as an ideal transformer plus a series loss.

of the line impedance by the method of Wheeler [7] and using the observed effective dielectric constant gave values of ~ 38 Ω.

Since the ring had only one port, the resonance was measured via the reflected power. The circuits were measured using a Hewlett Packard 8510 network analyzer with a WR-28, Ka-band waveguide option. Transition from the waveguide mode to the microstrip was accomplished by a cosine tapered *E*-plane ridge in a section of WR-28 waveguide [8]. The ridge contacted the end of the microstrip feedline at the edge of the substrate and launched the quasi-TEM microstrip mode. A standard waveguide calibration was performed at the plane where the tapered ridge fixture was connected. This calibration was performed at room temperature only and was assumed to be valid over the entire temperature range. Measurements were made using a closed-cycle helium refrigerator with a vacuum enclosure around the cold finger. Sample temperatures could be controlled from room temperature to between 10 K and 20 K. Normal signal levels at the calibration plane were 0.45 mW; however the level could be varied from 0.10 to 10 mW for study of the power dependence of the HTS film properties.

The reflection data from the resonators provided a measure of the loaded *Q*; the unloaded *Q*'s were calculated from these data using the model shown in Fig. 2 [9], where the ring resonance is modeled as a simple *RLC* circuit and the coupling gap as an ideal transformer with series loss. By circuit analysis of the model, the impedance of the isolated ring, and its Q (the unloaded Q or Q_0) is found to be

$$Z_{\text{res}} = \left[\frac{1}{R} + j\left(\omega C - \frac{1}{\omega L}\right)\right]^{-1} \tag{1}$$

$$Q_0 = \omega_0 CR \tag{2}$$

where ω is the angular frequency, ω_0 the resonant frequency, and R, C, and L the distributed resistance, capacitance, and inductance of the line. This represents the impedance and Q of the ring only, unperturbed by the input line. The loaded Q, the quantity actually measured, is the response of the ring loaded by the line impedance and coupling loss as transformed by the coupling gap. The impedance of this equivalent circuit and its Q_L (the loaded Q) is

$$Z_{\text{loaded}} = \left[\frac{n^2}{(Z_0 + R_L)} + \frac{1}{R} + j\left(\omega C - \frac{1}{\omega L}\right)\right]^{-1} \tag{3}$$

$$Q_L = \frac{\omega_0 CR(1+\sigma)}{(1+\sigma+\kappa)} = \frac{Q_0(1+\sigma)}{(1+\sigma+\kappa)} \tag{4}$$

where $\sigma = R_L/Z_0$ and $\kappa = Rn^2/Z_0$. The values of σ and κ relating the loaded and unloaded Q's can be determined from the reflection coefficient of the resonator. Far from the resonance, the reflection coefficient is given by

$$\Gamma = \frac{(\sigma - 1)}{(\sigma + 1)} \tag{5}$$

while at resonance

$$\Gamma = \frac{(\sigma + \kappa - 1)}{(\sigma + \kappa + 1)}. \tag{6}$$

Using the values of σ and κ obtained through Γ at these points and the measured loaded Q, the unloaded Q was determined using (4). The determination of whether the resonator was overcoupled or undercoupled was made from an examination of the Smith chart.

III. Circuit Performance

A. Resonator Q and Surface Resistance

Several superconducting resonators were fabricated and tested. In all cases the YBCO resonators showed no resonance above T_c owing to the high normal state resistivity of the YBCO material. At a point a few degrees below T_c, low-Q resonances appeared which quickly sharpened and rose above the unloaded Q values measured for gold resonators at those temperatures. The temperature at which the crossover between the superconducting resonator and the gold resonator occurred was dependent on the quality of the superconducting film, with the film T_c being a first-order indicator of the quality. Unloaded Q's for the superconducting resonators

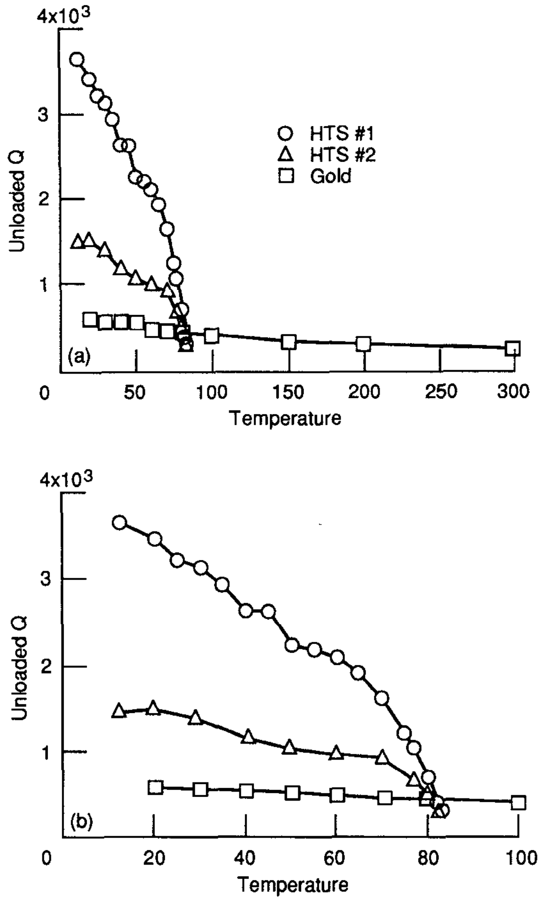

Fig. 3. Measured Q values for gold and superconducting resonators over the range (a) 0 to 300 K and (b) 0 to 100 K. The Q of the gold resonator increases by only a factor of 2 in cooling from 300 K to 20 K. The superconducting resonators show only marginal improvement over the gold resonator at 77 K, while operation at lower temperatures provides more substantial improvement.

continued to rise with decreasing temperature, though at a decreasing rate. Fig. 3 shows the unloaded Q versus temperature between 0 and 300 K (a) and 0 and 100 K (b) for two superconducting resonators and a gold resonator. The difference in the Q values between samples HTS#1 and HTS#2 is typical of the spread among the many superconducting resonators that were measured. Circuit performance ranged from only slightly better than gold across a wide temperature range to the best results as shown for HTS#1. A strong correlation was observed between the unloaded Q values and the film T_c [10]; films with higher T_c's generally had higher Q's. Film T_c's included in this study ranged from ~ 84 to 89 K.

The effect of the microwave drive power on the Q of superconducting films HTS#1 and HTS#2 is shown in parts (a) and (b) of Fig. 4, respectively, where the Q is plotted versus the microwave input power at three temperatures. The microwave power, as measured at the calibration plane, was varied from 0.25 mW to 10 mW. It is seen that there is no degradation in the performance for either film for this range of powers. In general, the laser-ablated films tended to show no power dependence up to at least 10 mW unless the film was of particularly

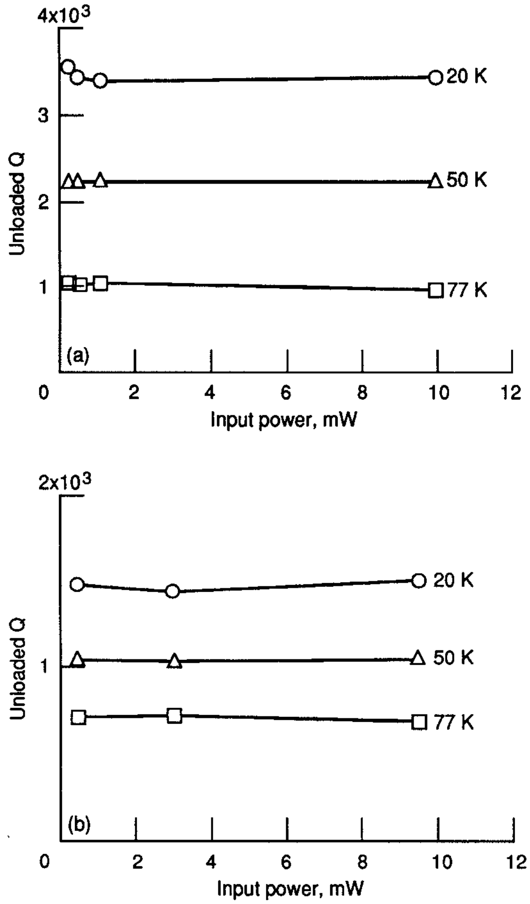

Fig. 4. Dependence of the superconducting resonator Q on the microwave input power for (a) HTS#1 and (b) HTS#2. The laser-ablated films did not show any power dependence.

low quality (i.e., $T_c < 80$ K and/or poor morphology).

The performance of the superconducting resonators, as shown in Fig. 3, provides some improvement over the gold circuit, with a factor of 2 increase in the unloaded Q at 77 K which grows to a factor of 7 at 20 K. This level of improvement is below the levels reported for X-band resonators, where order of magnitude improvements at 77 K are reported [11]. However, when the f^2 dependence of the superconducting surface resistance is considered, it is seen that smaller improvements over normal metal circuits are expected at higher frequencies. To assess the magnitude of the observed improvements and to determine whether better performance may be expected, modeling of the microstrip is necessary to account for the superconductor surface resistance. Such a model will not only allow prediction of circuit performance given the surface resistance; it will also allow the surface resistance to be inferred from measured Q data. The development of accurate equations for the superconducting microstrips is limited by the lack of precise values for the dielectric constant and loss tangent of the $LaAlO_3$ substrates and because the accuracy of existing closed-form expressions for microstrip structures is unknown when applied to high-dielectric-constant substrates such as $LaAlO_3$. Nevertheless, by matching experimental results from thin gold circuits where the surface resistance is reasonably known, sufficiently accurate expressions may be found to model the superconducting strips. For this work we have used the PEM [12].

The basis of the PEM method is that the internal impedance of the conductors (meaning the resistance and reactance arising from the field penetration into the strip and ground plane) can be calculated as the product of the surface impedance of the material, a geometric factor (G) determined by the line geometry, and a corrective term for the conductor thickness:

$$Z_{\text{internal}} = Z_{\text{surface}} \cdot G \cdot \coth[\tau t_e]. \tag{7}$$

Separate G factors are calculated for the strip and ground plane. The thickness correction for the strip is calculated from an effective thickness for the conductor, t_e, and a complex decay constant, τ, which accounts for the field decay into the conductor. These are calculated as

$$t_e = G \times (\text{cross-sectional area of strip})$$

$$\tau = (j\omega\mu\sigma)^{1/2}$$

where μ is the permeability of vacuum and σ the complex conductivity. The thickness correction for the ground plane is determined from the actual conductor thickness and the decay constant, τ. The geometric factors for the strip and ground plane are calculated by the incremental inductance rule [13]:

$$G = \frac{1}{\mu} \sum_i \frac{\partial L}{\partial n_i} \tag{8}$$

where $\partial L / \partial n$ is the derivative of the external inductance with respect to an incremental recession of the wall i.

We have used the equations of [11] to calculate the G factors for the strip and ground plane:

$$G_{\text{strip}} = \frac{2}{2\pi d} \cdot \left[1 - \left[\frac{w}{4d}\right]^2\right] \cdot \left[\frac{1}{2} + \frac{d}{w} + \frac{d}{\pi w} \ln(2d/t)\right] \tag{9}$$

$$G_{\text{ground}} = \frac{1}{2\pi d} \cdot \left[1 - \left[\frac{w}{4d}\right]^2\right] \tag{10}$$

where d is the substrate thickness, w is the strip width, and t is the conductor thickness. Q's were calculated by the standard formula:

$$Q = \frac{\beta}{2\alpha} = \frac{\beta}{2(\alpha_{\text{conductor}} + \alpha_{\text{dielectric}} + \alpha_{\text{radiation}})}. \tag{11}$$

The $\alpha_{\text{conductor}}$ is computed from the real part of the internal impedance as calculated from the PEM. The $\alpha_{\text{dielectric}}$ is computed from the expression [11]

$$\alpha_{\text{dielectric}} = \frac{27.3}{8.68} \cdot \left[\frac{qk}{k_{\text{eff}}}\right] \cdot \frac{\tan\delta}{\lambda_g} \qquad \left[\frac{\text{nepers}}{\text{meters}}\right]$$

$$q = \left[\frac{k_{\text{eff}} - 1}{k - 1}\right] \tag{12}$$

where k is the dielectric constant of the substrate and k_{eff}

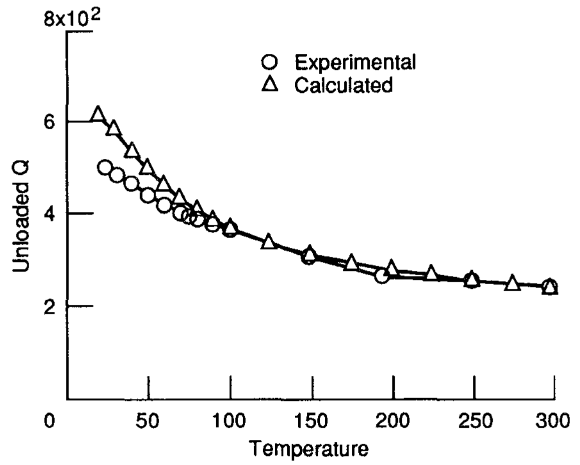

Fig. 5. Measured Q values for a thin gold resonator and values calculated using PEM. The agreement is within 10% to about 100 K. Increasing deviation below 100 K is due to errors in the calculated R_s value for gold at those temperatures.

is the effective dielectric constant experienced by the propagating wave. The radiation loss is assumed to be negligible owing to shielding of the circuit. Values for β were determined experimentally from the resonant frequency of the ring and the known circumference.

As a test of the PEM method, the Q values were calculated for a thin gold resonator (1 μm thick gold) and compared with the experimentally determined values. The dc resistivity of the gold in the ring was measured across the temperature range using a four point probe technique. The values of the resistivity were then used to calculate the microwave surface resistance (R_s) and penetration depth (δ_s) at the different temperatures using $R_s = (\omega\mu/2\sigma)^{1/2}$ and $\delta_s = (2/\omega\mu\sigma)^{1/2}$. A value of 8.3E-5 was used for the dielectric loss tangent. The results of the calculation are shown in Fig. 5. The match is within 10% across most of the temperature range, with increasing deviation below 100 K. Comparisons between experimental and computed values for 0.45 and 1.5 μm thick gold resonators also showed agreement within 10% above 100 K with increasing deviation below. The larger deviations at low temperatures do not appear to be a defect of the model, but rather appear to derive from incorrect values for the surface resistance of the gold. Nonidealities such as surface scattering are not accounted for by the simple surface resistance equation used, and probably result in an underestimation of the actual surface resistance. Thus the PEM equations adequately model the losses for the microstrip structure.

The PEM method was next applied to the superconducting resonator results using R_s values for the gold ground plane that were corrected to match the gold resonator experimental results below 100 K. The same value for tan δ as used in the gold resonator calculations was used here. Calculations were done with three values of the penetration depth, since this parameter is not known with a high degree of certainty. (Calculations in the following section give a value of approximately 3000 Å.) The results are summarized in Table I, where we see that R_s values computed at 77 K for HTS#1 lie in the range from 12 mΩ to 7 mΩ, and those for HTS#2 from 15 mΩ to 6 mΩ. These computed values of R_s at 77 K are somewhat higher than those for the best reported films (1–4 mΩ) [1]. If surface resistance values of the order of the best reported can be achieved in patterned strips, then better circuit performance than observed here can be achieved.

TABLE I
MICROWAVE SURFACE RESISTIVITY COMPUTED FROM THE SUPERCONDUCTING RESONATOR Q VALUES USING PEM

	HTS#1: 0° Penetration Depth, λ_0		
	1500 Å	3000 Å	4500 Å
20°	1 mΩ	0.8 mΩ	0.7 mΩ
50°	3.4 mΩ	2.9 mΩ	2.5 mΩ
77°	12 mΩ	9 mΩ	7 mΩ
	HTS#2: 0° Penetration Depth, λ_0		
	1500 Å	3000 Å	4500 Å
20°	7 mΩ	5 mΩ	3.7 mΩ
50°	10.4 mΩ	7.1 mΩ	5.5 mΩ
77°	15 mΩ	9.1 mΩ	6.3 mΩ

To determine the levels of performance possible in this circuit, the PEM can be used to calculate projected Q values. If a best value of $R_s = 1$ mΩ at 77 K is assumed and the present gold ground plane retained, a circuit Q of ~ 2500 is calculated, a factor of 5 higher than that for the all-gold circuit. The gold ground plane, in this case, limits the circuit Q. To achieve higher circuit Q's a superconducting ground plane is needed. If the gold ground is replaced with a 1 mΩ superconductor the Q rises to ~ 5000, an order of magnitude higher than for the gold circuit. Thus an order of magnitude improvement is possible at 77 K if surface resistivities of ~ 1 mΩ can be achieved and superconducting strips and ground planes are used. It should be noted, though, that this R_s value of 1 mΩ at 77 K, 35 GHz represents the lowest reported value for current YBCO material. For superconducting films with surface resistances higher than this, operation at lower temperatures would be necessary to achieve comparable improvements. The effect of the dielectric loss (assuming tan δ = 8.3E-5), while not dominant for the above conditions, is comparable in magnitude ($\alpha_{\text{dielectric}}$ = 0.12 nepers/meter) to the conductor losses and contributes to the total Q by an amount that cannot be neglected. As the conductor losses decrease, because of either improved film quality or lower operating temperature, the dielectric loss becomes dominant and will begin to limit the circuit performance.

B. Resonant Frequency Shift and Penetration Depth

Fig. 6 shows the resonant frequency as a function of temperature for both a superconducting ring and a gold ring. It is seen that both circuits undergo a shift in the resonant frequency to higher values as the temperature is decreased. The resonant frequencies do not coincide in the common temperature range of the two films owing to scatter in the substrate thicknesses among samples as well as differences in the line widths (a consequence of minor undercutting during etching). The magnitude of the shift for both the superconducting ring and the gold ring is of the order of 1% for the temperature range over which each circuit is operational. For the superconducting circuit, there is a very rapid change just below T_c and any practical circuit operating in this region would be susceptible to drift with any thermal fluctuations. Such drift would be most severely felt in narrow-band circuits or applications requiring a high degree of stability. Operation at 77 K is on the edge of this region and may or may not provide adequate stability depending on the requirements of the circuit.

The causes for the resonance shifts are different for the two circuits. The gold circuit has been analyzed with the data available on lanthanum aluminate, and the resonance shift was found to correspond to that which would be expected from the thermal contraction in the substrate. The shift of the superconducting resonator is due mostly to the change in the magnetic penetration depth in the superconducting strip with temperature, although other effects, among them thermal contraction, are embedded in the response also. By analysis of the frequency shift it is possible to extract a value for the penetration depth.

As a first approximation in this analysis, it is assumed that the shift of the superconducting resonator is due entirely to the changing penetration depth. The penetration depth affects the resonant frequency through the distributed inductance of the line. Specifically, the changing field penetration in the conductors results in a change in the internal reactance of the line. The resonant frequency may be related to the inductance through the standard expression for the propagation constant of a transmission line:

$$\beta = \frac{2\pi}{\lambda_g} = 2\pi f(LC)^{1/2}$$

where λ_g is the guide wavelength, f the frequency, and L and C the distributed inductance and capacitance of the line. For the ring resonator at resonance, we know that the circumference (D) is equal to an integral number of wavelengths (for this resonator, $n=3$); thus,

$$\lambda_g = D/3 \quad \text{and} \quad f_0\{T\} = \frac{3}{D\{T\}} \cdot \frac{1}{(L\{T\}C\{T\})^{1/2}} \tag{13}$$

where f_0 is the resonant frequency and the notation "$\{T\}$" denotes that the terms are functions of temperature. If we call $f_0\{0\}$ the resonant frequency at 0 K, then

$$\frac{f_0\{T\}}{f_0\{0\}} = \frac{D\{0\}(L\{0\}C\{0\})^{1/2}}{D\{T\}(L\{T\}C\{T\})^{1/2}}. \tag{14}$$

As a first-order approximation we assume that $C\{T\} = C\{0\}$ and $D\{T\} = D\{0\}$; i.e., we ignore any thermal contraction

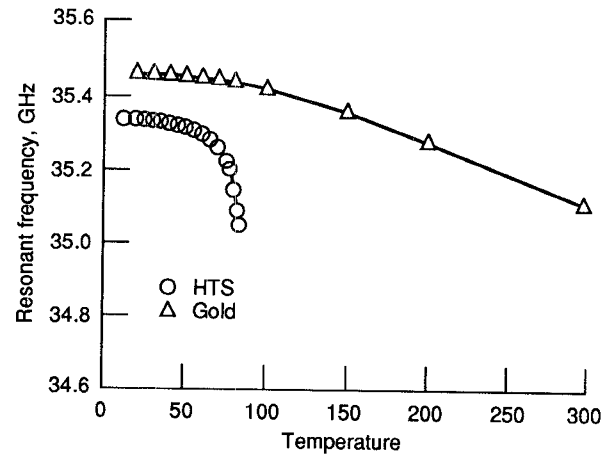

Fig. 6. The resonant frequency as a function of temperature for superconducting and gold resonators. The shift in the gold resonator is due mostly to thermal contraction in the substrate. The shift in the superconducting resonator is primarily due to the changing magnetic penetration depth with temperature.

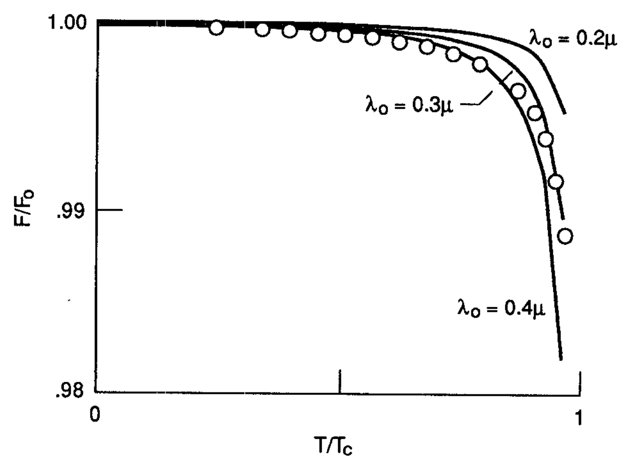

Fig. 7. Analysis to determine the penetration depth. The best fit to the experimental points gives a value of 3000 Å for the penetration depth.

in the substrate. Then

$$\frac{f_0\{T\}}{f_0\{0\}} = \left[\frac{L\{0\}}{L\{T\}}\right]^{1/2}. \tag{15}$$

Now the inductance of the transmission line is composed of three components, from the fields external to the conductors and the fields inside the strip and ground plane. The inductance due to the penetration into the strip and ground is attained from the imaginary part of the internal impedance as calculated from the PEM (preceding section). The expression used for the external inductance is the one that formed the basis for calculating the G factors in the PEM [13]:

$$L_e = \frac{\mu_0}{2\pi}\left[\ln(8d/w) + \frac{1}{32}(w/d)^2\right]. \tag{16}$$

An analysis for HTS#1 is shown in Fig. 7. The best fit to the data gives a λ_0 value of 3000 Å; similar analysis for HTS#2 also gave a value of ~3000 Å.

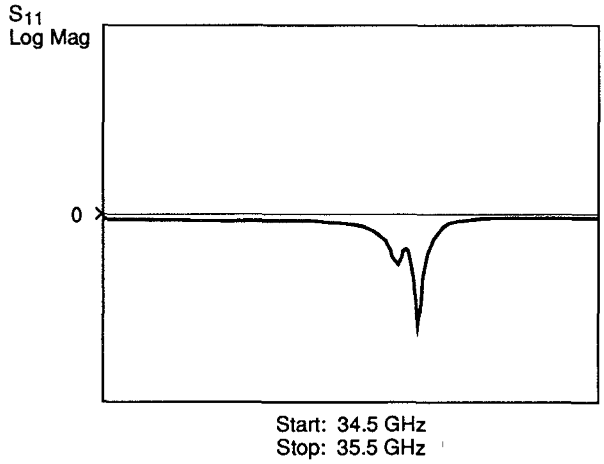

Fig. 8. An example of the double resonance that was seen in several superconducting resonators. The appearance of two peaks can be explained by an discontinuity within the ring. This discontinuity may be due to inhomogeneities in the superconducting film or in the substrate.

C. Double Resonances in Superconducting Rings

A phenomenon seen in superconducting resonators several times in the course of this study was the splitting of the single resonance peak into two or more overlapping peaks, as illustrated in Fig. 8. Analysis of such resonators was hampered because the overlapping resonances did not allow Q values to be calculated with a degree of accuracy. The splitting of a ring resonance can be explained by a discontinuity in some region of the ring [14]. This discontinuity can be in either the HTS film or the substrate, but in either case it will set up standing waves which vary slightly in frequency, thus producing two closely spaced resonance peaks. Examination in an optical microscope of the superconducting resonators that showed the splitting did not reveal any obvious defects in the strip. The lanthanum aluminate substrates contain a large number of twins and it is possible that the splitting may be traced to this. At this point, however, no clear determination of the cause can be arrived at. It can only be noted that superconducting films, including films that otherwise appear of high quality, are susceptible to regions of inhomogeneity that can produce such discontinuities. It should be pointed out that similar effects will not be seen in linear resonators since a discontinuity would divide the line into two smaller sections that would show resonances at frequencies above the primary resonance of the line and so be missed.

IV. Conclusions

Microstrip ring resonators with YBCO superconducting strips and gold ground planes have been fabricated and tested at 35 GHz. These circuits showed higher unloaded Q's than identical resonators with gold strips and ground planes; the best circuit achieved a factor of 2 improvement at 77 K and reached a factor of 7 improvement at 20 K. Because of the f^2 dependence of the superconductor surface resistance, smaller relative improvements over normal metal circuits are expected at millimeter-wave frequencies. However, modeling using PEM indicated an R_s value of ~ 10 mΩ at 77 K, which is higher than the best reported value of 1–4 mΩ at that frequency and temperature. This indicates that improvements in circuit performance over those observed here are possible if patterned strips exhibiting lower surface resistance can be fabricated. To achieve an order-of-magnitude increase in unloaded Q at 77 K over the normal metal circuit, calculations suggest that a normal ground plane cannot be used. If both strip and ground were superconducting material with an R_s of 1 mΩ, which represents the lowest values reported to date at 35 GHz and 77 K, then an order-of-magnitude improvement at 77 K would be possible.

Observation of the resonant frequency versus temperature of the superconducting resonator showed a shift of approximately 1% from just below T_c to 20 K. Operation at 77 K places the circuit away from the steepest part of the frequency versus temperature curve, but still on the "knee," indicating possible thermal stability problems for very narrow band circuits operated at that point. An analysis of the frequency shift indicated a value of 3000 Å for the effective penetration depth, λ_0^*.

Millimeter-wave superconducting circuits were found to severely test the quality of superconducting films. To achieve significant improvements in loss characteristics over normal metal lines at these frequencies, the highest quality films and/or operation below 77 K are required.

References

[1] H. Piel and G. Muller, "The microwave surface impedance of high-T_c superconductors," *IEEE Trans. Magn.*, vol. 27, pp. 854–862, Mar. 1991.

[2] D. B. Rensch *et al.*, "Fabrication and characterization of high-T_c superconducting X-band resonators and bandpass filters," *IEEE Trans. Magn.*, vol. 27, pp. 2553–2556, Mar. 1991.

[3] R. C. Hansen, "Superconducting antennas," *IEEE Trans. Aerosp. Electron. Syst.*, vol. 26, pp. 345–355, Mar. 1990.

[4] N. Klein *et al.*, "Millimeter wave surface resistance of epitaxially grown $YBa_2Cu_3O_{7-x}$ thin films," *Appl. Phys. Lett.*, vol., 54, pp. 757–759, Feb. 1989.

[5] F. A. Miranda, W. L. Gordon, K. B. Bhasin, J. D. Warner, and G. J. Valco, "Millimeter wave transmission studies of $YBa_2Cu_3O_{7-x}$ thin films in the 26.5 to 40 GHz frequency range," in *Superconductivity and applications*, H. S. Kwok *et al.*, Eds. New York: Plenum Press, 1990, pp. 163–167.

[6] A. A. Valenzuela and P. Russer, "High Q coplanar transmission line resonator of $YBa_2Cu_3O_{7-x}$ on MgO," *Appl. Phys. Lett.*, vol. 55, no. 10, pp. 1029–1031, Sept. 1989.

[7] K. C. Gupta, R. Garg, and I. J. Bahl, *Microstrip Lines and Slotlines.* Norwood, MA: Artech House, 1979, pp. 7–13.

[8] R. R. Romanofsky and K. A. Shalkhauser, "Universal test fixture for monolithic mm-wave integrated circuits calibrated with an augmented TRD algorithm," NASA Technical Paper, TP-2875, Mar. 1989.

[9] E. L. Ginzton, *Microwave Measurements.* New York: McGraw-Hill, 1957, pp. 391–434.

[10] C. M. Chorey *et al.*, "An experimental study of high T_c superconducting microstrip transmission lines at 35 GHz and the effect of film morphology," *IEEE Trans. Magn.*, vol. 27, pp. 2940–2943, Mar. 1991.

[11] P. A. Polakos, C. E. Rice, M. V. Schneider, and R. Trambarulo, "Electrical characteristics of thin-film $Ba_2YCu_3O_{7-x}$ supercon-

ducting ring resonators," *IEEE Microwave and Guided Wave Lett.*, vol. 1, pp. 54–56, Mar. 1991.

[12] H. Y. Lee and T. Itoh, "Phenomenological loss equivalence method for planar quasi-TEM transmission lines with a thin normal conductor or superconductor," *IEEE Trans. Microwave Theory Tech.*, vol. 37, pp. 1904–1909, Dec. 1989.

[13] R. A. Pucel, D. J. Masse, and C. P. Hartwig, "Losses in microstrip," *IEEE Trans. Microwave Theory Tech.*, vol. MTT-16, pp. 342–350, 1968; correction, vol. MTT-16, p. 1064, 1968.

[14] N. J. Rohrer *et al.*, "Sequentially evaporated thin film $YBa_2Cu_3O_{7-x}$ superconducting microwave ring resonator," in *Proc. Conf. Science and Technology of Thin Film Superconductors* (Denver CO), May 1990.

Christopher M. Chorey (M'89) received the B.S. degree in electrical engineering in 1984 and the M.S. degree in materials science in 1987 from Case Western Reserve University.

Since 1988 he has been with Sverdrup Technology at NASA's Lewis Research Center, where he is studying microwave applications of high-temperature superconductors and cryogenic-temperature microwave active devices.

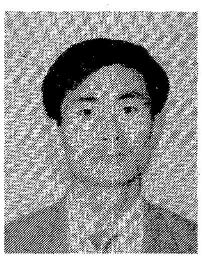

Keon-Shik Kong (S'88) was born in Seoul, Korea, on January 27, 1964. He received the B.S. and M.S. degrees in electrical and computer engineering from the University of Texas at Austin in December 1986 and December 1988, respectively. He is currently working toward the Ph.D. degree at the University of Texas at Austin. His current research deals with the application of superconductors in microwave circuits. In 1985, he obtained an Engineering Scholar Award from General Dynamics. Mr. Kong is a member of Tau Beta Pi and Eta Kappa Nu.

Kul B. Bhasin (S'74–M'83–SM'89) received the M.S. and Ph.D. degrees from Purdue University and the University of Missouri-Rolla, respectively.

Since 1983 he has been a Senior Research Scientist in the Solid State Technology Branch of the Space Electronics Division of the NASA Lewis Research Center in Cleveland, OH. Prior to joining NASA he was with Gould, Inc., from 1977 to 1983.

He is currently engaged in the development of GaAs microwave devices and circuits, microwave photonics, and superconducting elecronics for space application.

Dr. Bhasin has authored many publications and he coedited the book *Microwave Integrated Circuits*. He has been the recipient of the IR-100 Award, the NASA Group Achievement Award, and the Gould Scientific Achievement Award. Dr. Bhasin is on the editorial board of the *Microwave and Optical Technology Letters*. He is a member of APS and Sigma Xi.

J. D. Warner, photograph and biography not available at the time of publication.

Tatsuo Itoh (S'69–M'69–SM'74–F'82) received the Ph.D. degree in electrical engineering from the University of Illinois, Urbana in 1969.

From September 1966 to April 1976, he was with the Electrical Engineering Department, University of Illinois. From April 1976 to August 1977, he was a Senior Research Engineer in the Radio Physics Laboratory, SRI International, Menlo Park, CA. From August 1977 to June 1978, he was an Associate Professor at the University of Kentucky, Lexington. In July 1978, he joined the faculty at the University of Texas at Austin, where he became a Professor of Electrical Engineering in 1981 and Director of the Electrical Engineering Research Laboratory in 1984. During the summer of 1979, he was a Guest Researcher at AEG-Telefunken, Ulm, Germany. In September 1983, he was selected to hold the Hayden Head Centennial Professorship of Engineering at the University of Texas. In September 1984, he was appointed Associate Chairman for Research and Planning of the Electrical and Computer Engineering Department at the University of Texas. In January 1991, he joined the University of California, Los Angeles, as Professor of Electrical Engineering and holder of the TRW Endowed Chair in Microwave and Millimeter Wave Electronics.

Dr. Itoh is a member of the Institute of Electronics and Communication Engineers of Japan, Sigma Xi, and Commissions B and D of USNC/URSI. He served as the Editor of the IEEE TRANSACTIONS ON MICROWAVE THEORY AND TECHNIQUES for the years 1983–1985. He serves on the Administrative Committee of the IEEE Microwave Theory and Techniques Society. He was Vice President of the Microwave Theory and Techniques Society in 1989 and President in 1990. He is Editor-in-Chief of the IEEE MICROWAVE AND GUIDED WAVE LETTERS. He was Chairman of USNC/URSI Commission D from 1988 to 1990 and is Vice Chairman of Commission D of the International URSI. Dr. Itoh is a Professional Engineer registered in the state of Texas.